JOURNAL OF APPLIED POLYMER SCIENCE VOL. 19, PP. 683–695 (1975)

Porous Polymer Carbons. I. Preparation and Properties of Porous Poly(vinylidene Chloride) Precursor Copolymers

G. J. HOWARD and S. KNUTTON,* *Department of Polymer and Fibre Science, University of Manchester Institute of Science & Technology, Manchester M60 1QD, England*

Synopsis

A series of porous solids has been prepared by the suspension polymerization of mixtures of vinylidene chloride and ethylene glycol dimethacrylate with a nonsolvating diluent. Alteration of the monomer composition and concentration leads to marked variations in the total porosity and pore sizes of the solid polymers. Scanning electron microscopy shows that the suspension-polymerized beads consist of a microglobular interior encapsulated in a more coherent outer skin. This surface material affects the apparent density of the polymers and their behavior in mercury intrusion porosimetry and low-temperature nitrogen adsorption.

INTRODUCTION

The synthesis of porous solids by the polymerization of suitable monomers is well established. Where the material is destined for an application such as ion exchange or gel permeation chromatography, suspension polymerization is a particularly convenient technique since it produces the product in the form of small beads. In applications such as those mentioned, it is necessary to include crosslinking comonomers to provide the polymer with adequate mechanical strength and solvent resistance. The nature and extent of the internal porosity is largely determined by the diluent (which may be solvating, nonsolvating, or macromolecular) incorporated into the disperse phase of the suspension polymerization. Much of the literature on porous polymers refers to styrene–divinylbenzene copolymers,[1–4] although other systems have been described.[5] However, so far as we are aware, there are no reports on the formation of porous polymers which are suitable precursors for carbons or on their carbonization. For the present paper, we describe the synthesis and characterization of porous bead polymers based on vinylidene chloride.

EXPERIMENTAL

Vinylidene chloride (Koch Light Ltd) was redistilled immediately prior to polymerization; inhibitor was removed from the crosslinking comonomer, ethylene glycol dimethacrylate, by adsorption into silica gel. The radical generator

* Present address: The Grammar School, Mexborough, Yorkshire, England.

for the polymerization was benzoyl peroxide which was recrystallized from chloroform/methanol at room temperature. Carbon tetrachloride and toluene were of Analar quality and were not further purified. The required combination of monomers was mixed with the desired volume of diluent, which was a 3:1 toluene:carbon tetrachloride mixture; in all polymerizations the benzoyl peroxide content was 0.5 wt-% on total monomer. The organic phase was vigorously dispersed in an aqueous solution of methylcellulose and this suspension then thickened by the addition of a concentrated aqueous solution of locust bean gum (Indalka A, Ellis Jones & Co). Polymerization was carried out in sealed bottles following the technique developed by Pepper.[6] After filling, the heavy-walled bottles (Coca-Cola) were capped, placed in a double-walled steel container acting as an explosion shield, and polymerization carried out in an oven at 55° for 48 hr. The polymerization vessels were then cooled, cautiously opened, and 4-*tert*-butylcatechol was added as a radical scavenger. The suspension stabilizer and the thickening agent were hydrolyzed with warm, dilute hydrochloric acid and the beads exhaustively washed, first with further acid and subsequently with water. To ensure displacement of the diluent, the beads were soaked in acetone overnight, washed, and dried in vacuo at 50° for several days.

The product designation is as follows. A coding letter is followed by the volume fraction of crosslinking comonomer in the monomer mixture, while the final figure gives the volume fraction of diluent in the total organic phase. Thus, A/.500/.750 is a polymer made from equal volumes of vinylidene chloride and ethylene glycol dimethacrylate, with three volumes of diluent to one of total monomer. Some samples were lightly ground in a mortar; these are distinguished by a suffix G to the coding. Most preparations yielded beads of ca. 0.5 mm in diameter; however, the homopolymer (B/0/0) beads were about an order of magnitude smaller.

The apparent particle density was determined pyknometrically with mercury as containing fluid; the pyknometer was filled under a light vacuum (ca. 1 torr). Polymer densities were determined by helium displacement using a gas adsorption apparatus; this was a volumetric apparatus of conventional design[7] which was also employed to determine both B.E.T. surface areas (N_2 and CO_2) and full sorption–desorption isotherms (N_2). For this work, a preliminary outgassing at 10^{-5} torr and 100°C was carried out for 2 hr; a higher outgassing temperature could not, of course, be used with these thermally unstable polymers. Mercury porosimetry determinations were performed on a Carlo Erba porosimeter at the laboratories of the British Coke Research Association. Analysis was carried out up to pressures corresponding to the filling of pores of dimensions equivalent to hollow cylinders of 75 Å radius. The scanning electron microscopy was made on silver-coated (vacuum evaporation) samples in a Stereoscan instrument (Cambridge Instruments); highly porous samples sometimes exhibited charging effects despite the conducting coating.

RESULTS

Total pore volumes of the polymers were estimated (Table I) by comparison of the specific volumes measured in mercury and helium, respectively, i.e.,

$$\text{pore volume} = (\rho_{Hg})^{-1} - (\rho_{He})^{-1}. \quad (1)$$

TABLE I
Pore Volumes[a] of Polymer Beads by Equation (1)

Polymer	Whole beads			Lightly ground beads		
	ρ_{Hg}	ρ_{He}	Pore volume	ρ_{Hg}	ρ_{He}	Pore volume
B/.250/.000	1.38	1.58	0.07	1.33	—	0.09
B/.250/.250	1.23	1.52	0.16	1.24	—	0.15
B/.250/.333	1.06	1.54	0.29	0.97	—	0.37
B/.250/.400	0.91	1.49	0.44	0.85	—	0.52
B/.250/.500	0.77	1.42	0.64	0.74	—	0.69
B/.250/.750	0.69	1.55	0.79	0.74	—	0.69
B/.160/.400	1.27	—	0.13	—	—	—
B/.080/.400	1.35	—	0.08	—	—	—
C/.160/.490	0.92	—	0.43	—	—	—

[a] In cm^3/g; calculated with mean $\rho_{He} = 1.52$.

TABLE II
Pore Volumes[a] by Mercury Intrusion

Polymer	Whole beads	Lightly ground beads
B/.250/.000	0.06	—
B/.250/.250	0.22	0.21
B/.250/.333	0.30	0.40
B/.250/.400	0.58	0.60
B/.250/.500	0.86	0.66
B/.250/.750	1.07	—
B/.160/.400	0.19	—
B/.080/.400	0.10	—

[a] In cm^3/g.

A crosslinked bead formed in the absence of diluent has little internal volume not available to mercury at atmospheric pressure; that is, any internal pores are open and mostly very large. At constant crosslinker contents, increase of the diluent fraction during polymerization brings about a progressive increase in porosity. At constant diluent, the porosity increases sharply with crosslinker content. The pore volumes quoted in Table I are calculated on the basis of a constant helium density, and it is assumed that helium is unadsorbed by the polymer at room temperature. The slight trend to lower helium densities with diluent content, if real, is not readily explained; lower values could result from closed pores or from lower degrees of crystallinity. Some samples were ground to open up interior structures. If the polymer samples had closed macropores, or if the bead surface restricted ingress of mercury, the result of a gentle grinding should be to increase the apparent density in mercury and give a lower pore volume. Generally, however, the change is in the opposite direction.

Other estimates of pore volume are obtained from data derived from mercury porosity (Table II). In the present work, the maximum pressure of 1000 atm means that internal volume in pores of equivalent radii less than 75 Å is excluded, as are macropores greater than 75000 Å radius since these are filled by mercury at atmospheric pressure. For whole beads, the intrusion pore volumes tend to be greater than the values obtained from density differences, despite the exclusion of

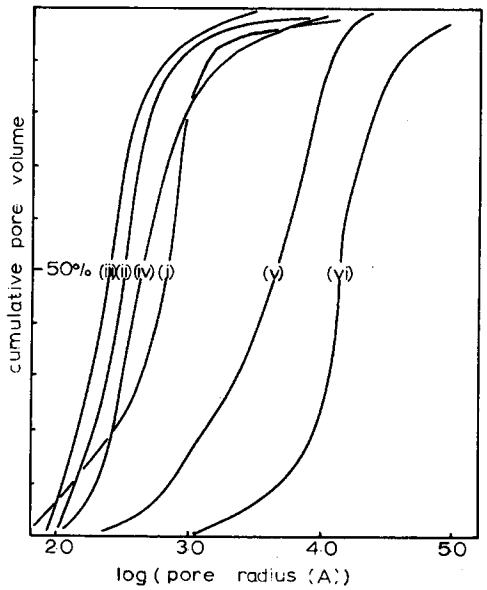

Fig. 1. Pore size distributions by mercury intrusion porosimetry. Whole beads, crosslinker volume fraction 0.250; diluent contents (i) zero; (ii) 0.250; (iii) 0.333; (iv) 0.400; (v) 0.500; (vi) 0.750.

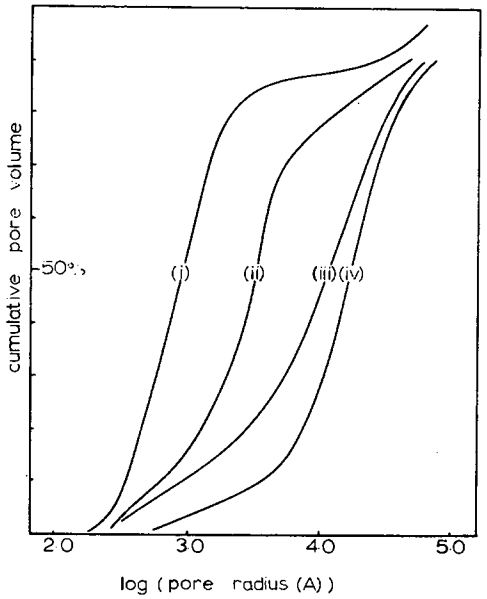

Fig. 2. Pore size distributions by mercury intrusion porosimetry. Ground beads, crosslinker volume fraction 0.250; diluent contents (i) 0.250; (ii) 0.333; (iii) 0.400; (iv) 0.500.

small pores; the discrepancy widens as the beads take on a more open structure but is not so evident with the ground beads.

Pore size distributions from mercury intrusion porosimetry are shown for whole beads in Figure 1 and for fractured beads in Figure 2. Figure 3 compares polymers made with differing crosslink densities. Mean pore radii (that is, at

TABLE III
Mean Pore Radii[a] by Mercury Intrusion

Polymer	Whole Beads	Lightly Ground Beads
B/.250/.000	675	—
B/.250/.250	320	875
B/.250/.333	240	3350
B/.250/.400	450	12300
B/.250/.500	4400	16000
B/.250/.750	14000	—

[a] In Å.

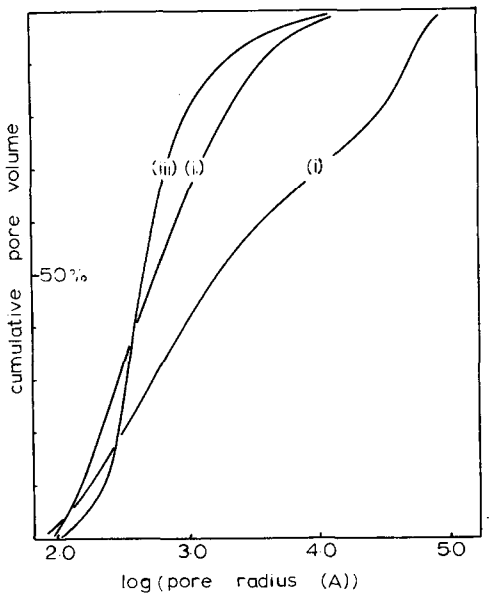

Fig. 3. Pore size distributions by mercury intrusion porosimetry. Whole beads, diluent volume fraction 0.400; crosslinker contents (i) 0.080; (ii) 0.160; (iii) 0.250.

half total filling of pores) are given in Table III. With whole beads, the apparent pore size at first decreases with diluent content at polymerization, the trend being reversed at higher diluent volume fractions. At low crosslinker contents, the pores are noticeably larger. Except for the two most porous polymers, the mercury intrusion data suggest that there may be a small amount of internal pore volume in pores of equivalent radii smaller than 75 Å. However, if structural breakdown, particularly of whole beads, occurs during the mercury intrusion process, the experimentally obtained distribution curves will have been displaced to lower pore dimensions, especially at higher pressures. Certainly, previously partially fractured samples give altered pore size curves in which the mean radii increase monotonically with diluent content and which show evidence of a fraction of large pores and an absence of pores smaller than ca. 150 Å equivalent radius. Repeatability is quite good, except at the higher intrusion pressures.

Two effects must be considered in comparing the pore size distributions of the whole and fractured beads. The first effect is that of structural breakdown during measurement; that a degree of breakdown takes place is shown by the follow-

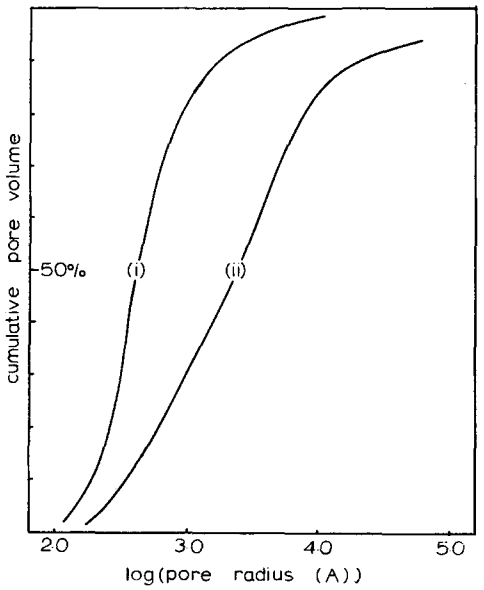

Fig. 4. Pore size distributions by mercury intrusion porosimetry. B/.250/.400: (i) original determination; (ii) redetermination.

ing experiment. A relatively porous polymer (B/.250/.400) was filled with mercury at 1000 atm and the pressure relaxed to atmospheric; mercury remaining trapped in the specimen was removed with nitric acid and the intrusion measurement repeated. The result (Fig. 4) is a considerable displacement of the pore size distribution curve: however, no gross, permanent deformation is observed, the density in mercury is almost unchanged, and the beads retain their spheroidal appearance. A second effect is the influence of the surface structure of the bead. This, if different to the interior, would largely determine the measured pore size distribution for whole beads whereas the distributions found from ground beads would be more typical of their interior morphology.

Further elucidation of the exterior and interior structures is provided by scanning electron microscopy. Figures 5a to 5c show whole, crosslinked beads. A spherical bead is produced at a low diluent content (B/.250/.250); the photomicrograph is of a bead that had been sliced with a razor blade. Beads prepared at higher diluent contents show evidence of gross collapse (Fig. 5b) which may become severe (Fig. 5c); this collapse is presumed to occur during the latter stages of polymerization.

The external surface of the polymer beads (Figs. 6a–6e) shows a gradation of appearance. Poly(vinylidene chloride) homopolymer, polymerized without diluent, has an outer surface with open pores with diameters of 10^3–10^4 Å (Fig. 6a). Crosslinked copolymers made with lower volume fractions of diluent have no such openings (6b,6c) although in the latter case (B/.250/.333), a large, and atypical, cracked region in the surface provides evidence of a porous interior structure. The more porous sample (B/.250./500) exhibits an external surface which is different in the ridges and depressions (6d,6e). Clear evidence of the skin structures on the crosslinked copolymer beads is illustrated in Figures 7a–7e which are of bead interiors or edges revealed by fracturing. The skin structure

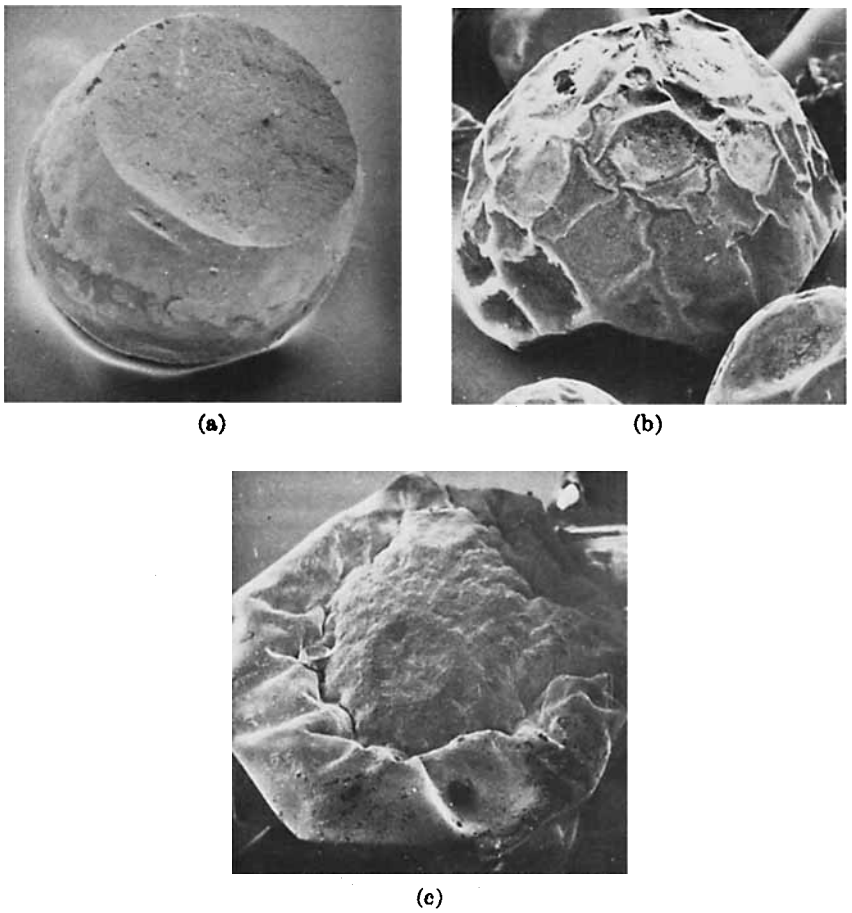

Fig. 5. Scanning electron microscopy of whole beads: (a) B/.250/.250 (×34); (b) B/.250/.500 (×94); (c) B/.250/.750 (×120).

is relatively thin (ca. 3000 Å), often less than the average diameter of the microspheres formed in the interior. The property changes alluded to previously, which occur when beads are gently fractured, must result in part from the existence of this largely continuous skin structure on the "as polymerized" beads.

Indirect evidence of the peripheral structure of whole beads was also obtained by qualitative adsorption from methanolic methylene blue solution. Whole beads adsorbed little, whereas fractured beads took up considerable quantities of dye; in the latter case, a slight but consistent color difference could be seen between the original bead surface and the fracture surface. Similarly, the rate of color development with alcoholic sodium hydroxide showed significant differences. The small particles of homopolymer turned black in some 12 hr, fractured copolymer beads became dark brown in a few days, while whole copolymer beads required several weeks to reach this color. The darkening at equilibrium dehydrochlorination varies with copolymer composition since the lengths of conjugated sequences that may be produced are limited by the crosslinker residues.

The scanning electron micrographs show that the interior of a copolymer bead is comprised of an agglomeration of microglobules. The size of these basic

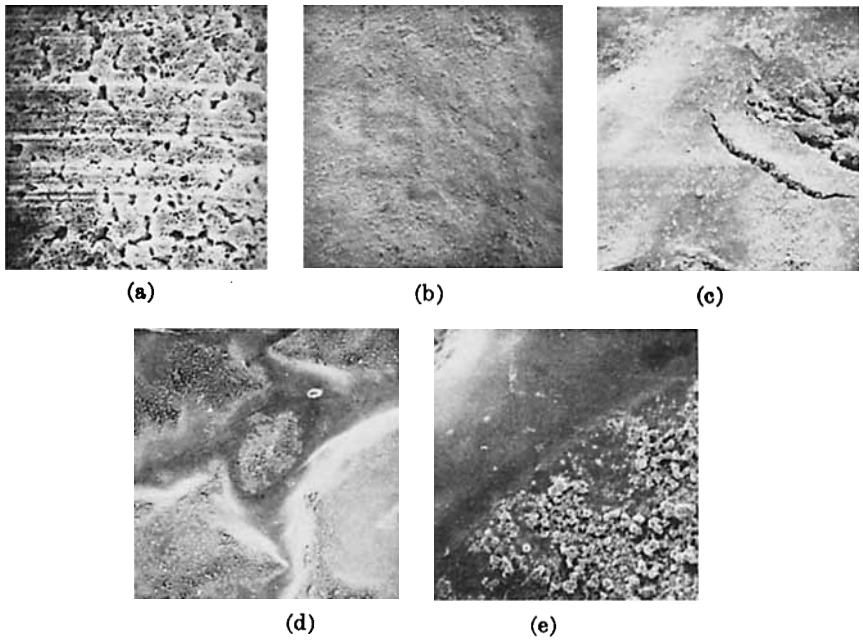

Fig. 6. Scanning electron microscopy of polymer beads: outer surfaces (a) B/.000/.000 (×690); (b) B/.250/.250 (×880); (c) B/.250/.333 (×710); (d) B/.250/500 (×322); (e) B/.250/.500 (×1610).

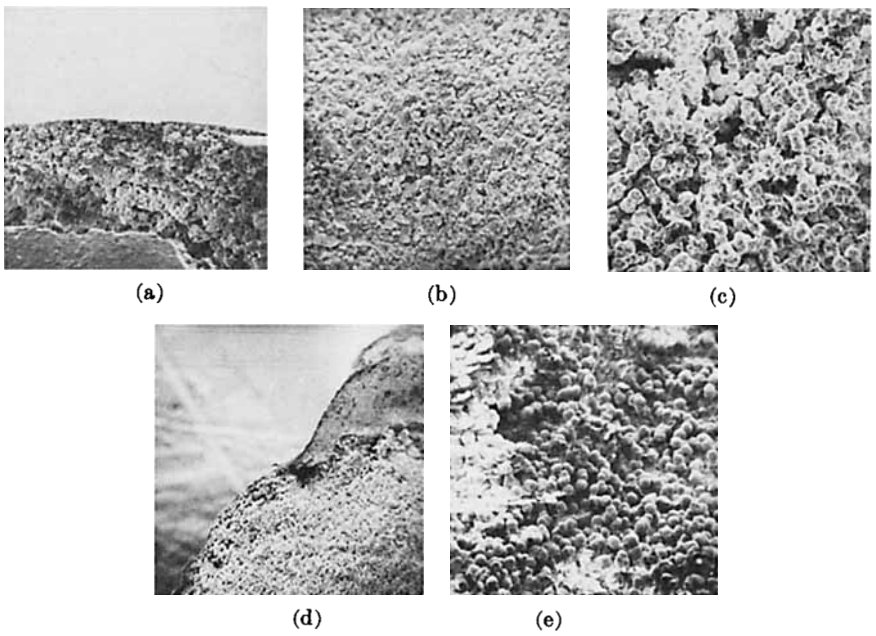

Fig. 7. Scanning microscopy of polymer beads: interiors and edges (a) B/.250/.250 (×876); (b) B/.250/.333 (×610); (c) B/.250/.500 (×650); (d) B/.250/.500 (×96); (e) B/.250/.750 (×770).

TABLE IV
Mean Radii[a] of Interior Microglobules

Polymer	Radius
B/.250/.250	2200
B/.250/.333	4300
B/.250/.400	5400
B/.250/.500	10900
B/.250/.750	10000

[a] In Å.

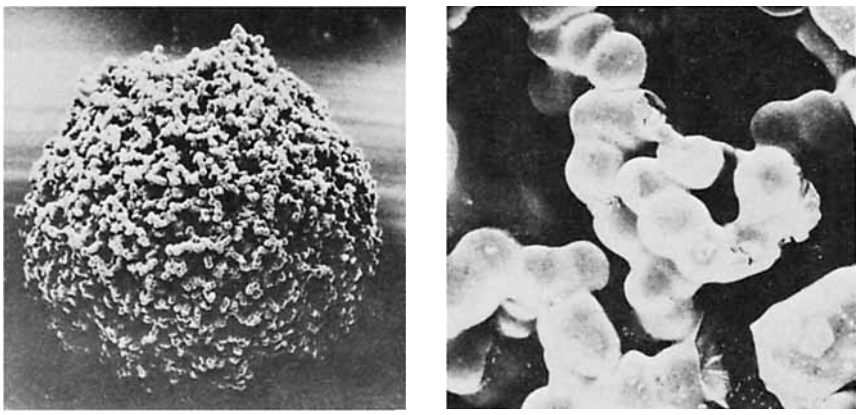

(a) (b)

Fig. 8. Scanning electron microscopy of ion exchange resin (IRA-938) (a) ×114; (b) ×1110.

structural elements is given in Table IV; sample B/.250/.000 has a fine structure that could not be resolved well enough to estimate the microglobular diameter.

Although the interior structure is similar in form to that of styrene–divinylbenzene copolymers, the microspheres may be much larger in the latter example. Figure 8 shows a scanning electron micrograph of a commercial macroreticular ion exchange resin (Amberlite IRA 938) in which the microglobules are ca. 25000 Å in radius. This is, however, not a typical styrene–divinylbenzene macroporous resin but is an example similar to micrographs published by Kunin[8] and, incidentally, shows no skin structure.

A limited amount of electron microscopy in the transmission mode was undertaken, but considerable difficulties in sample preparation were encountered; the microtome knife, whether of glass or diamond, tended to fracture the open structure and to push together the microglobular sections. The micrographs shown in Figures 9a to 9c illustrate the larger microglobule sizes as diluent content is increased; microsphere radii measured for B/.250/.333 and B./250/.500 agree completely with those estimated from scanning electron microscopy.

Sorption–desorption isotherms with N_2 at 77°K were performed with several whole-copolymer bead samples. Low-pressure hysteresis is shown (Fig. 10a), a phenomenon usually[9] attributed to intercalation. However, most examples of intercalation involve adsorbates having a greater interaction with the adsorbent than would be expected for nitrogen at 77°K with an organic, partially crystalline polymer well below its glass transition. Most interestingly, the low-pressure

TABLE V
Surface Areas[a] of Suspension-Polymerized Samples

Polymer	BET (N_2)	S.E.M.	Mercury intrusion	Volume/radius ratio
B/.250/.250G	4.7	9.0	5.4	4.3
B/.250/.333G	3.1	4.6	3.9	2.3
B/.250/.400G	1.9	3.7	3.5	1.2
B/.250/.500G	2.2	1.8	1.9	1.0
B/.250/.750G	1.9	2.0	—	—
B/.000/.000	11.9	—	—	—

[a] In m^2/g.

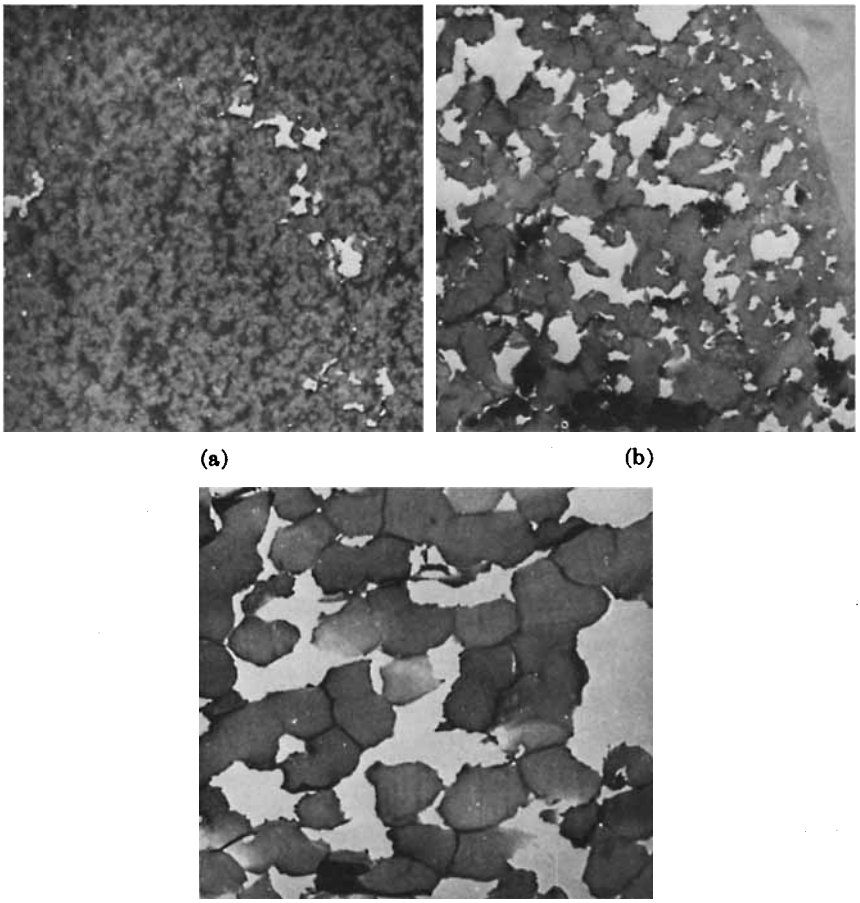

(a) (b)

(c)

Fig. 9. Transmission electron microscopy of polymer beads: (a) B/.250/.000 (×4350); (b) B/.250/.333 (×4350); (c) B/.250/.500 (×4350).

hysteresis is not shown by fractured beads (e.g., Fig. 10b); such samples have a "normal" hysteresis loop typical of a solid with transitional porosity. This loss of low-pressure hysteresis on fracturing the polymers implies that the phenomenon in this case results not from intercalation but from activated diffusion in the skin structure of whole beads.

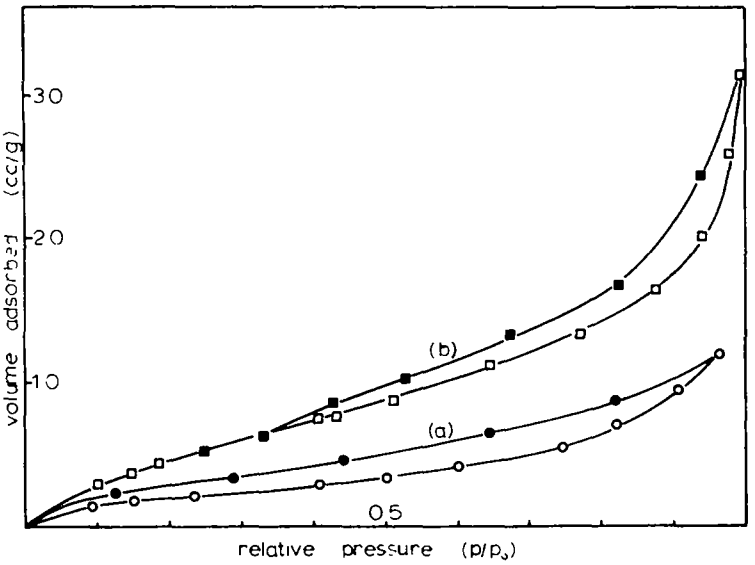

Fig. 10. Adsorption isotherms. N_2, 77°K: (a) B/.250/.500; (b) B/.250/.500 G.

Apparent surface areas were found from the nitrogen adsorption data (BET); the data for ground copolymer beads only were considered, but the value for unground poly(vinylidene chloride) homopolymer is also included in Table V. Surface areas were also estimated as the total surface of microglobules from the electron microscopic radii; from mercury penetration data, by the method due to Orr;[10] and from the pore volume/pore radius ratio, assuming cylindrical pores.

Considering the many implicit assumptions and the low level of the surface areas, the agreement between methods is acceptable.

DISCUSSION

Each droplet in the suspension polymerization is a separate polymerization reaction: a solution copolymerization in which the polymeric product is insoluble in the liquid of the droplet. The morphological features of the final polymer particles are determined by the conditions of polymerization, in this case by the diluent content and the composition of the mixed monomers. The monomer reactivity ratios in the copolymerization of vinylidene chloride and ethylene glycol dimethacrylate have not been reported, but the Q,e values of the Alfrey-Price scheme[11] are available;[12] the reactivity ratios calculated from the Q,e parameters are $r(VDC) = 0.24$, $r(EGDM) = 4.1$. This means that the polymer formed initially will be relatively rich in the dimethacrylate. The copolymers have been described in terms of the overall composition of the polymerization system. However, when larger quantities of diluent are present and the rate of polymerization consequently reduced, the products may fall somewhat short of 100% conversion. Indeed, the measured chlorine content of the B/.250/— series decreases slightly as the diluent is increased; further, the accord with the expected value is better at lower crosslinker contents. Thus, some of the structural features attributed solely to the diluent content may result in part from a progressive, if slight, increase of the dimethacrylate content in the final copolymer. To an extent, however, this trend to higher effective crosslink den-

sities in the more porous samples will be mitigated by the increased extent of intramolecular crosslinking and the greater amount of chain transfer that will have taken place at higher diluent contents.

Not all the pore volume and pore size data are readily explicable. There is evidence that high-pressure mercury porosimetry produces concomitant structural changes. Further, there are large changes in apparent pore size distributions between whole and fractured samples. Whatever the absolute validity of the estimations of pore dimensions, it is evident that changes in the polymerization recipe (crosslinker and diluent) lead to very considerable differences; for example, the mean pore radius of B/.250/.500G is some twenty times that of B/.250/.250G.

The indirect evidence for a bead surface which differs in structure to the interior is substantiated by the nitrogen isotherms where the skin is implicated in the low pressure hysteresis behavior. How the activated diffusion held responsible for this hysteresis is produced by a skin which, to judge from porosimetry data, has some openings much larger than the probe gas molecules is open to conjecture.

The scanning electron-microscopic investigations not only confirm the existence of a skin on each suspension-polymerized particle but demonstrate the microglobular nature of the interior. These structural features require to be explained. Poly(vinylidene chloride) is soluble in only a limited number of highly polar solvents, and then usually at elevated temperatures; it is insoluble in its monomer. Thus, polymerization in the bulk phase or in solvents for the monomer becomes heterogeneous. Wessling and Harrison[13] have shown that, in the bulk homopolymerization of vinylidene chloride, polymer precipitates as crystallites from the beginning of the reaction and that subsequent growth is at the crystallite surfaces. In the copolymerizations considered here, the dimethacrylate units impede crystallization. Nonetheless, wide-angle x-ray diffraction shows that incorporation of 0.250 volume fraction of crosslinker does not entirely destroy the high crystallinity of the homopolymer. Of course, the compositional drift during copolymerization will lead to the formation of vinylidene chloride-rich (and hence crystallizable) material toward the final stages of reaction.

No skin is formed on vinylidene chloride homopolymer beads; its formation cannot, therefore, be related to the adsorbed suspension stabilizers but is, rather, to be attributed to the comonomer. The following hypothesis is advanced; first-formed copolymer is relatively high in dimethacrylate units and contains some unreacted ethylenic unsaturation. This material is probably well swollen by the reaction medium but is also hydrophilic relative to the droplet so that it will accumulate at the interface because of preferential wetting, having a lower contact angle with the aqueous than with the reaction phase. Continuation of this process will soon obliterate the original interface (the skin represents less than 1% of the bead mass) and terminate the transport away from the interior. Further reaction in the bulk of the bead will take the familiar form of a heterogeneous polymerization in somewhat swollen microglobules while continued reaction in the surface will produce a more densely crosslinked, and hence less porous, structure. A generally similar explanation has been advanced by Heitz[14] to account for the skin observed in a vinyl acetate/divinyl adipate copolymerization; skin structures have also been reported[1] in styrene–divinylbenzene copolymerizations carried out under special conditions.

One of the authors (S.K.) held a Science Research Council research studentship during the period of these studies (1968–71). The authors are indebted to the British Coke Research Association for the use of their mercury porosimeter and to Dr. J. W. Patrick of those laboratories for valuable advice.

References

1. J. C. Moore, *J. Polym. Sci., A-2,* 835 (1964).
2. J. R. Millar, D. G. Smith, W. E. Marr, and T. R. E. Kressman, *J. Chem. Soc.,* 218 (1963).
3. R. Kunin, E. F. Meitzner, and N. M. Bortnik, *J. Amer. Chem. Soc.,* **84,** 305 (1962).
4. J. Seidl, J. Malinsky, K. Dusek, and W. Heitz, *Fort. Hochpolym. Forsch.,* **5,** 113 (1967).
5. W. Heitz and K. L. Platt, *Makromol. Chem.,* **127,** 113 (1969).
6. K. W. Pepper, *J. Appl. Chem.,* **1,** 124 (1951).
7. V. T. Crowl, in *Particle Size Analysis,* Society of Analytical Chemistry, London, 1966, p. 288.
8. R. Kunin, in *Ion-Exchange in the Process Industries,* Society of Chemical Industry, London, 1970.
9. D. R. Everett, in *The Solid-Gas Interface,* E. A. Flood, Ed., Vol. 2, Arnold, London, 1967, p. 1055.
10. C. Orr, Jr., *Powder Technol.,* **3,** 117 (1969/70).
11. T. Alfrey, Jr., and C. C. Price, *J. Polym. Sci.,* **2,** 101 (1947).
12. J. Brandup & E. H. Immergut, Eds., *Polymer Handbook,* Interscience, New York, 1966.
13. R. A. Wessling and I. R. Harrison, *J. Polym. Sci. A-1,* **9,** 3471 (1971).
14. W. Heitz, *J. Chromatogr.,* **53,** 37 (1970).

Received July 14, 1974